

## Analysis of a preliminary configuration for a floating wind turbine

H.F. Wang<sup>\*1</sup>, Y.H. Fan<sup>1</sup> and Iñigo Moreno<sup>2</sup>

<sup>1</sup>*School of Natural Sciences and Humanities, Harbin Institute of Technology Shenzhen Graduate School, Shenzhen, China*

<sup>2</sup>*Polytechnic School, University of Burgos, Burgos, Spain*

*(Received November 6, 2015, Revised April 10, 2016, Accepted June 1, 2016)*

**Abstract.** There are many theoretical analyses and experimental studies of the hydrodynamics for the tension leg platform (TLP) of a floating wind turbine. However, there has been little research on the arrangement of the TLP's internal structure. In this study, a TLP model and a 5-MW wind turbine model as proposed by the Minstitute of Technology and the National Renewable Energy Laboratory have been adopted, respectively, to comprehensively analyze wind effects and wave and current combinations. The external additional coupling loads on the TLP and the effects of the loads on variables of the internal structure have been calculated. The study investigates preliminary layout parameters-namely, the thickness of the tension leg body, the contact mode of the top tower on the tension leg, the internal stiffening arrangement, and the formation of the spoke structure-and conducts sensitivity analyses of the TLP internal structure. Stress is found to be at a maximum at the top of the tension leg structure and the maximum stress has low sensitivity to the load application point. Different methods of reducing maximum stress have been researched and analyzed, and the effectiveness of these methods is analyzed. Filling of the spoke structure with concrete is discussed. Since the TLP structure for offshore wind power is still under early exploration, arrangements and the configuration of the internal structure, exploration and improvements are ongoing. With regard to its research and analysis process, this paper aims to guide future applications of tension leg structures for floating wind turbine.

**Keywords:** floating wind turbine; tension leg platform; structural design

---

### 1. Introduction

Because of steady and strong wind energy resources, ocean energy is one of the most reliable alternative energy sources for countries that have sufficiently large wind and wave resources, and offshore wind farms have become highly attractive as an ideal energy solution. China's potential ranks first in the world for offshore wind resources in the East Sea and the South Sea, which are close to the Guangdong wind energy deposit. However, in the South China Sea, most of the water is 50m deep, which means the traditional supporting structure is too expensive in this water field (Wang and Fan 2013). The US, northern Europe and Japan all face the same problem as China. In

---

\*Corresponding author, Ph.D., E-mail: [phdwhf@163.com](mailto:phdwhf@163.com)

order to deal with this challenge, floating supporting systems that have been developed from ocean engineering are being considered a key solution to make offshore wind farms a viable energy resource from an economic standpoint (Jonkman 2007).

There are many existing studies on tension leg platform floating offshore wind turbine systems (TLP-FOWTS). The first work in developing a TLP wind turbine system was performed by Withee in 2004 at MIT. Alina examined the dependencies between the design parameters and performance for TLP systems (Aina 2011). Withee (2004) researched fully coupled time-domain simulations for a TLP system in waves and wind. Suzuki (2009) designed a TLP system that could be used in Japan during earthquake conditions. Bae (2010) researched the dynamic response of a mini TLP-type offshore floating wind turbine. Nihei (2010) investigated the motion characteristics in waves and wind for the TLP wind turbine. Bachynski (2012) analyzed a wide range of parametric single-column TLP designs. Jonkman developed a new model to simulate the dynamic of offshore floating wind turbines, and used it to verify TLP systems (Jonkman 2009). Musial introduced a NREL TLP concept and presented a cost comparison between the Dutch tri-floater (semi-sub) and the NREL TLP based on supporting a generic 5-MW wind turbine. Wayman studied several different concepts, including barges and TLPs supporting the NREL 5-MW baseline offshore wind turbine (Wayman 2006, Wayman *et al.* 2006). Moon and Nordstrom (2010) provided a general overview of a TLP-type design concept and its environmental and design criteria. The TLP concept presented in this paper was designed to be a combination of guidelines and criteria considered to be suitable for an initial principle “working stress design” approach and a quick design cycle. Henderson (2010) proposed a TLP concept for German waters with consideration to technology principles, challenges and potential wind resources. In China research on a TLP floating structure for wind turbines is currently scant. Ren (2002a, b) introduced a floating structure considering tension leg and mooring lines, and also performed an experiment to test it. Zhao (2012) proposed a new tension leg platform foundation (Wind-Star TLP) to the NREL 5MW offshore wind turbine and studied motion characteristics under extreme conditions. Wang and Fan designed a new TLP model, called an HIT-Floating Offshore Wind Turbine-Tension Leg Platform (HIT-FOWT-TLP); larger diameters were considered for the spoke (Wang 2014). None of the previous research involves internal structural design for the tension leg of a wind turbine; Pietro’s thesis (2009) referred to the tension leg platform in ocean engineering and provides a kind of internal layout of the tension leg structure using the design method of a similar system in ocean engineering, and then carried out a finite element analysis for the arrangement of the tower and the tension leg. In conclusion, an offshore wind turbine is different from the conventional ocean platform structure with regard to external loads, operating conditions and integral structures, resulting in effects upon the design parameters of internal structures to be discussed in depth.

In this paper, the TLP model proposed by MIT with the 5MW wind turbine model from NREL have been adopted in comprehensive consideration of wind effects, as well as wave and current combinations to calculate the external additional coupling loads on the tension leg platform, thus analyzing the effects of these coupling loads upon the variables of the tension leg internal structure. The structure variables refer to the structural thickness of the tension leg, the treatment for top connection sections and internal transverse/vertical stiffening ribs, and the structural layout of the spoke.

## 2. Analysis input

Table 1 Environmental condition

Condition	Survival
Significant wave height- $H_s$	10
Peak wave period- $T_p$ (s)	17.64

## 2.1 NREL 5MW wind turbine model and TLP model

### 2.1.1 NREL 5MW wind turbine model

An NREL 5MW offshore wind turbine was used in this study, its preliminary concept designed by Jonkman (2009). The disadvantage of using this type of wind turbine is that it has already been adopted as a reference in earlier numerous scientific studies (Ren 2012a, Ren 2012b, Zhao *et al.* 2012, Wang *et al.* 2014, Pietro 2009). The NREL 5 MW baseline is a conventional upwind machine with three blades operating at variable speeds and variable pitch. The tower is a conventional tubular steel section with a variable radius starting from 6 m at the bottom to 3.6 m at the top.

### 2.1.2 NREL/MIT TLP model

The MIT/NREL is a floating W/T from modifications to a TLP made at the Massachusetts Institute of Technology (MIT); it consists of a cylindrical platform, ballasted with concrete and moored by four pairs of vertical tendons in tension; each pair of tendons attaches to a spoke that radiates horizontally from the bottom of the platform; the concrete ballast is used to ensure that the combined turbine platform system remains stable during float-out, even without the tendons, in mild met ocean conditions. Here we have selected a spoke length of 27 m (Matha 2010).

## 2.2 Environment and site data

The wind turbine installation location is on the coast. Environmental conditions that have been obtained from previous research (Jonkman *et al.* 2009) are shown in Table 1, because the depth varies, the installation site average depth of 200 m is considered in there. A wave spectrum is the distribution of wave energy in a function of frequency, which describes the total energy transmitted by a wave-field at a specific time. As one of the simplest, most widely used spectrums, the Pierson-Moskowitz is an empirical relationship between the energy distribution and frequency of irregular waves at sea. It is based upon the assumption that waves reach an equilibrium state, if the wind blows steadily for a long time over a large area, known as a fully developed sea wave. The energy density of wave is defined by Withee (2004) in the Pierson-Moskowitz spectrum as shown in Eq. (1)

$$S(\omega) = \pi^3 \left( \frac{2H_s}{T_z} \right)^2 \frac{1}{\omega^5} \exp \left[ -\pi^3 \left( \frac{2}{T_z \omega} \right)^4 \right] \quad (1)$$

$\omega$  is the wave frequency,  $H_s$  the significant wave height and  $T$  is the zero-crossing period. It has an equivalent equation based on the peak wave period definition between the peak wave period  $T_p$  and the zero crossing period (Matha 2010)

$$T_p = \left( \frac{5\pi}{4} \right)^{0.25} T_z \quad (2)$$

Table 2 Force and moment

Force & Moment	Date
$F_x$ (Kn)	846.26
$F_y$ (Kn)	3.16
$F_z$ (Kn)	0.64
$M_x$ (KnM)	183.53
$M_y$ (KnM)	50336.60

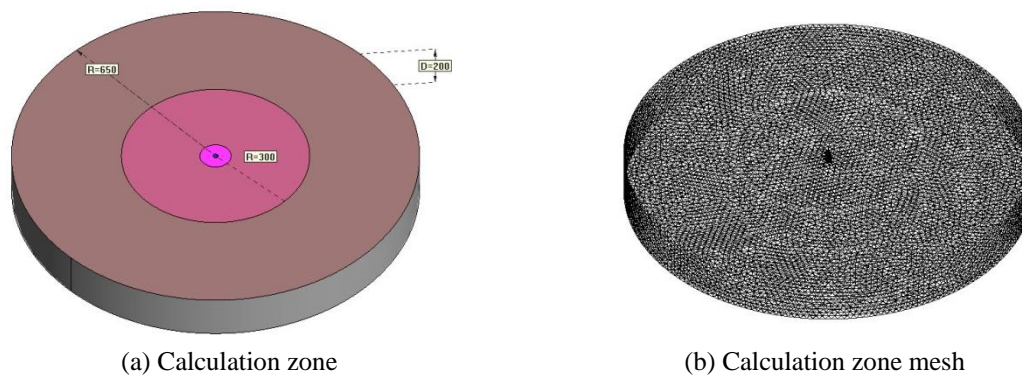


Fig. 1 Calculation zone model mesh

In Jordi's thesis (Torrás *et al.* 2011), the author calculated the external force applied to the tension leg structure and provided the external loads under different load combinations. Thus we selected a type of load combination in order to describe the calculation procedures in our calculation model in which consideration has been given to the external acting force, as seen in the table below:

### 2.3 TLP FEM model

Dimensions of the tension leg are as shown in the above table. Concrete was used to fill the cabin. The water depth remained consistent with the MIT model. In the first round of iterative calculations for the stress of the model, the structural design of the MIT-TLP concept mainly consisted of columns, pontoons, and column/pontoon nodes. The TLP hull was a fully welded steel structure that consisted of high-tensile steel with a minimum yield stress of 355 MPa. In addition, it was assumed that the initial thickness was 0.02 m. In the preliminary model, any extrinsic reinforcement measurement, e.g., horizontal stiffening rib, vertical stiffening rib and spoke, was not taken into consideration. Irrespective of the factors, the calculated stress may exceed the design strength of the material, but can still be used in an analytical study, since our purpose was to analyze the effects of factor changes on the stress. However, this was not used as an indispensable requirement required in deduction calculations. While calculating structural stress, the first seakeeping calculation & analysis was carried out where external winds, water currents and other loads could be imported into the structural calculation & analysis procedures. In these kinds of structural calculation models as shown in Fig. 1(a), water depth in the adopted computational domain is 200 m, the core computational domain has a radius of 300 m, and the

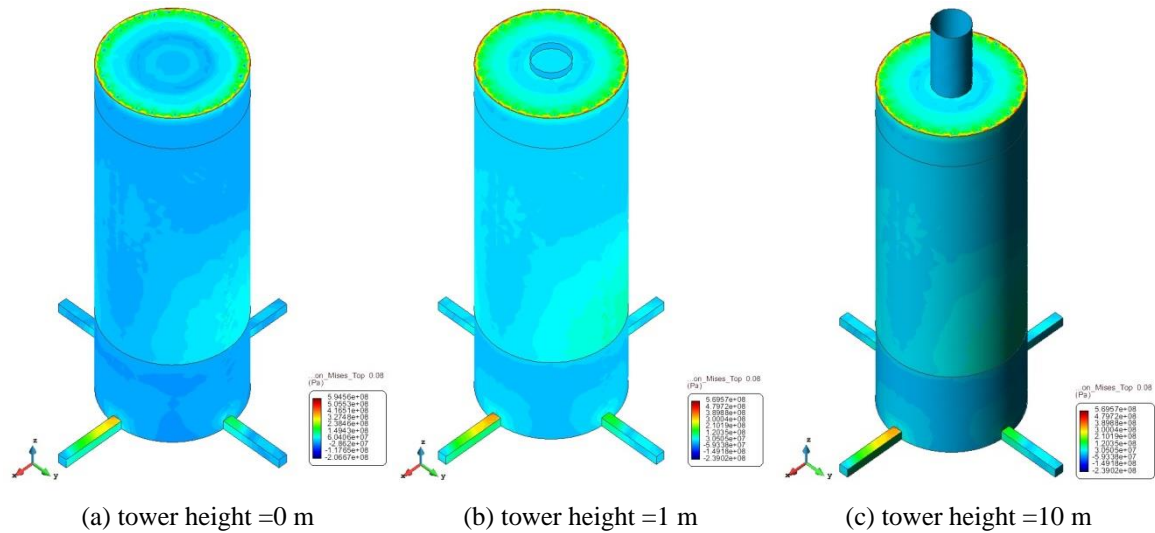


Fig. 2 The result for different tower height (thickness is 0.01 m)

whole computational domain has a radius of 650 m; the number of triangle elements are 22628, the number of tetrahedral elements are 363533, and the total nodes are 65283. For the units adopted by the NREL/MIT -TLP: Num. of linear elements=1324, Num. of triangle elements is 7633, Num. of tetrahedral elements is 32562, Num. of nodes is 10245.

### 3. Calculations and analysis

#### 3.1 Contact stress concentration between tower and main pontoon

In order to guarantee the maximum operating condition combinations obtained during calculation, the external wave-wind load combination as following: the external wave load was applied from a zero incidence direction, i.e., the incidence angle of wave was vertical to the plane where the wind turbine blade was located, and the external additional bending movement generated by the rotating wind turbine could be directly superposed with the external wave load.

First of all, in the case of the 0.02 m wall thickness, the stress nephogram obtained through calculation is as shown in Fig. 3 below where there is no internal support. The stress nephogram also shows that the maximum stress appears on the top, which received the maximum external force. Secondly, the maximum stress appearing at the top was due to the effects of load applying points is verified. A stress relief analysis by mounting three steel tower of 0, 1 m and 10 m high on the top is carried out. The comparison results show that the top stress is at its highest all the time under different circumstances, which are 213 Mpa, 207 Mpa and 200 Mpa respectively as shown in Fig. 3(a), (b), (c). Thirdly, in the case of the 0.01 m wall thickness, the stress concentration appears at the connection of the main pontoon and the spoke at the bottom as shown in Fig. 2; the stress there is 595 Mpa, 569 Mpa and 569 Mpa relative to the towers at different heights. The top stress concentration is not continuous, but rather periodical and discontinuous. As shown in Fig. 4, in the case of the 0.03 m wall thickness, the stress concentration falls rapidly but not disappearing,

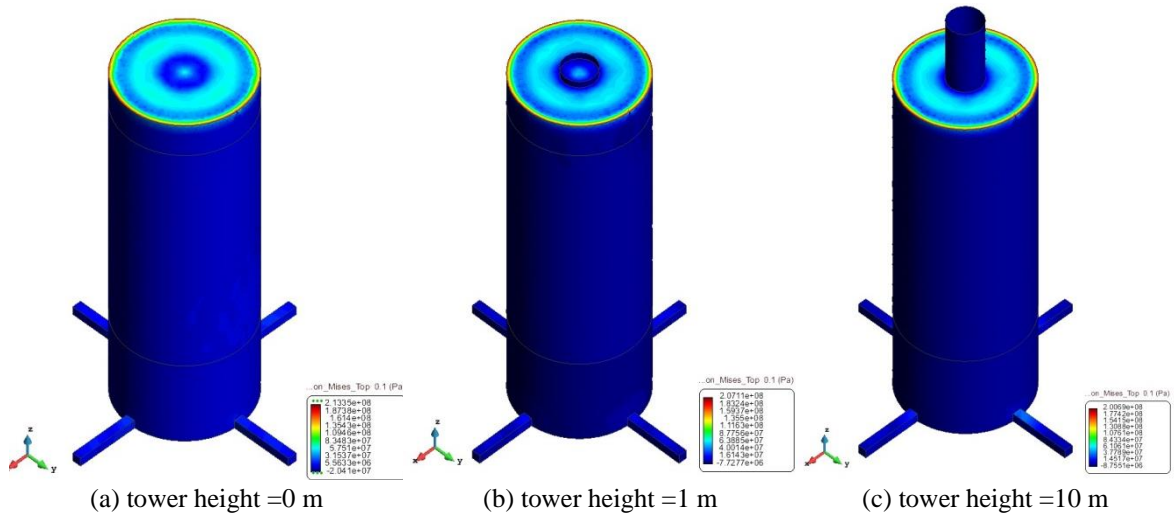


Fig. 3 The result for different tower height (thickness is 0.02 m)

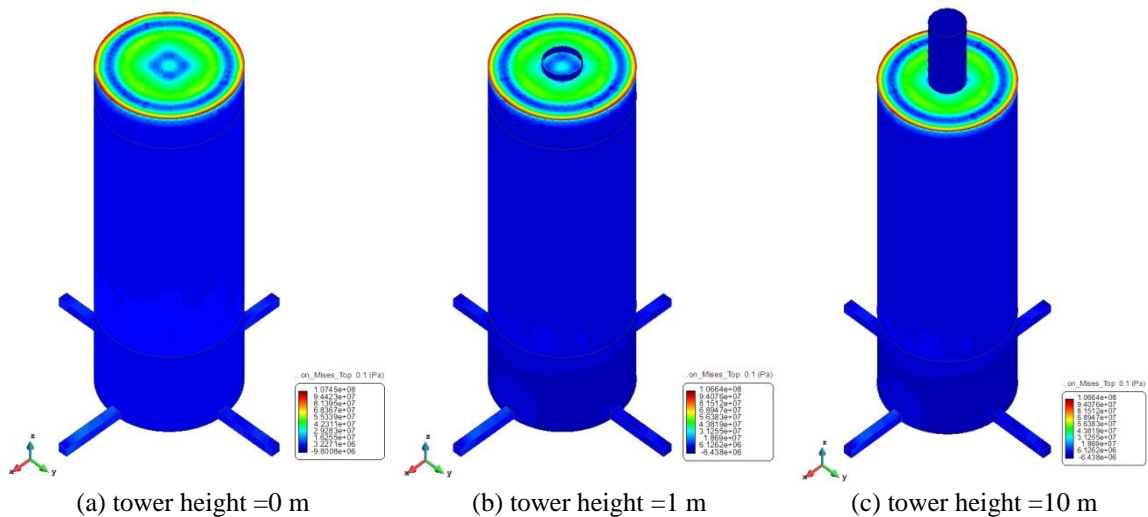


Fig. 4 The result for different tower height (thickness is 0.03 m)

that stress being 107 Mpa, 106.6 Mpa, 106.6 Mpa, relative to the towers at different heights. The effects of the tower to the stress concentration significantly reduce when compared with the phenomena occurring when the wall thickness is 0.01 m and 0.02 m. Data comparisons show that the maximum stress lowers by 369 MPa, namely 65%, when the thickness is doubled to 0.02 m. When the thickness is tripled to 0.03 m, the maximum stress lowers by 462 MPa, namely 81%, compared with when the wall thickness is 0.01 m; it lowers by 93 MPa, namely 47%, compared to when the wall thickness is 0.02 m. Therefore, it can be concluded that thickness changes have a great impact on the material stress, and thickness is also a key factor that determines overall cost. The issue of how to seek reasonable thicknesses and cost will constitute an important subject in the future. Changes in thickness will have great impact on the structural stress distribution, by which

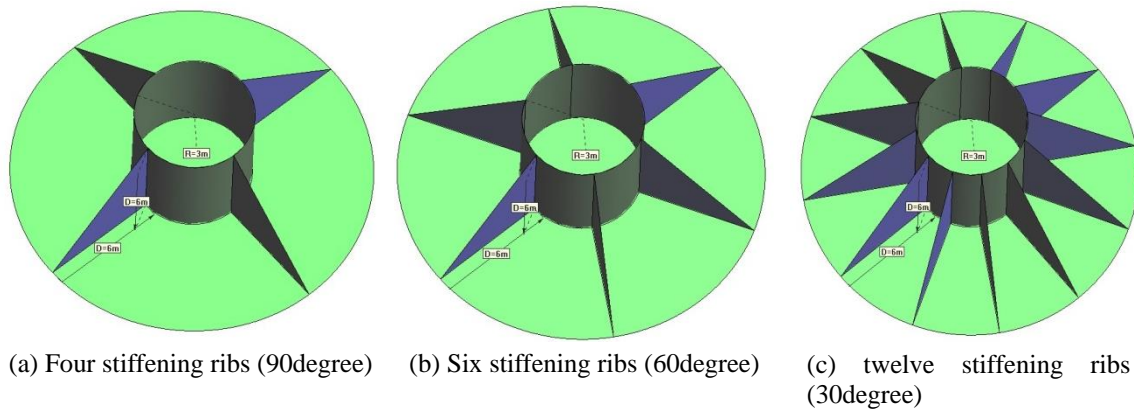


Fig. 5 Different stiffening rib

one can control stress concentration positions and allocate materials properly.

The above calculation and analysis show that the top, as a stress concentration area, requires subsequent local reinforcement and will not make the stress concentration disappear due to the tower rising. However, wall thickening will not only smooth out the maximum stress but will also result in a noteworthy reduction of the maximum stress, which is favorable to the utilization of materials. The maximum stress position will vary in the case of the lower thickness. A reasonable selection of thickness may adjust the position on the material where the maximum stress appears.

Though thickening functions can be used in the utilization of materials and the reduction of the maximum stress, doing so will also increase costs. In order to seek a better and more economic scheme, it is necessary to select a proper method to reduce the top stress concentrations at a certain thicknesses, so as to optimize the structure and reduce costs. Therefore, first considering the independent inclined stiffening rib around the connection of the tower and the main pontoon. The pontoon in the whole structure is 0.02 m thick; the standard thickness of an inclined stiffening rib is 0.02 m, and its height is the pontoon diameter minus the base diameter of the tower divided by 2. They are arranged at intervals of  $90^\circ$ ,  $60^\circ$  and  $30^\circ$ , which are shown in Fig. 5. In the external loads applied, wave load direction is vertical to the blade direction and parallel to the plane of one specific stiffening rib which load case can make the result obtain the maximum stress.

In the case of the 0.02 m thickness the maximum stress position and result nephogram were obtained under wave load as show in Fig. 6. Compared with the situation when the stiffening rib was not applied, the maximum stress increased and the stress concentration area reduced obviously, and was restricted to the contact area between the inclined stiffening rib and the top platform, i.e., the side of the main pontoon, shifting to the side but not at the top. In the case of the 0.02 m thickness, as for  $90^\circ$  inclined support, the top stress ranges from 238 MPa to 155 Mpa with 655 MPa as the maximum that appears at the connection between the side of the main pontoon and the inclined support which is shown in Fig. 6(a). As for the  $60^\circ$  inclined stiffening support, the main stress range and the maximum stress are equivalent to those at  $90^\circ$ . However, the maximum stress dispersion area was obviously reduced, which could be interpreted as when more supports share the external force, it reduces the stress to the individual supports. Regarding the  $30^\circ$  inclined stiffening rib support, the top stress ranged from 236 MPa to 153 MPa with 648 MPa as the maximum is shown in Fig. 6(c). Under a fixed thickness and a wave incident angle, more inclined supports significantly reduced the stress concentration area from the previous connection area

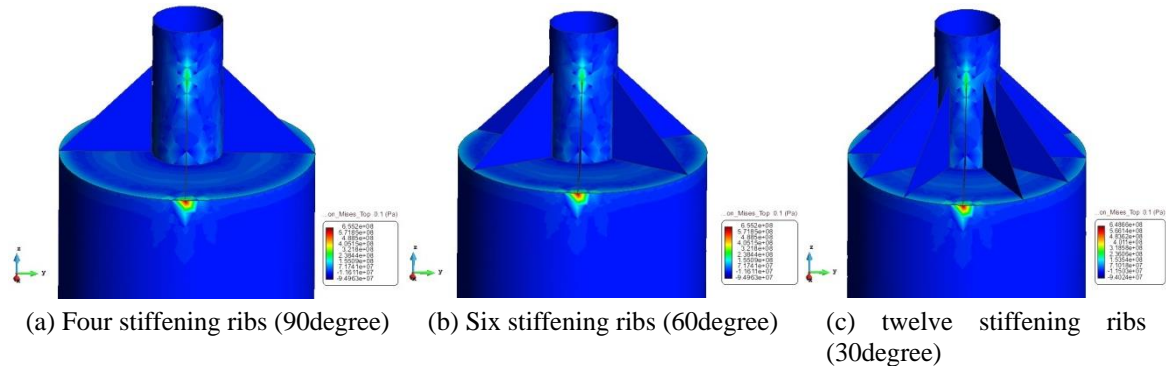


Fig. 6 The result for different ribs in load case 1 (thickness =0.02 m)

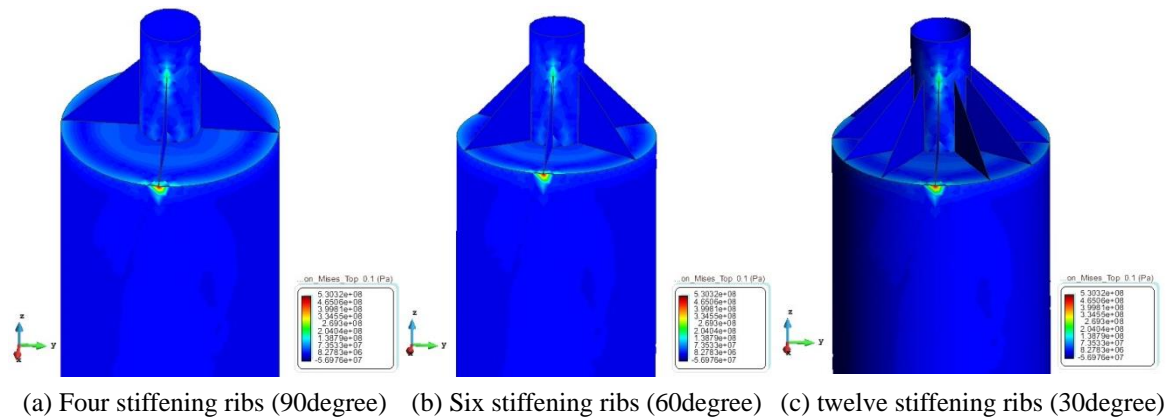


Fig. 7 The result for different ribs in load case 1 (thickness =0.03 m)

between the top and the outer wall of the pontoon to the connecting point between the inclined support and the outer wall of the pontoon, but increasing the stress concentration value.

Similarly, when the thickness was 0.01 m or 0.03 m, the stress result are calculated. The corresponding results show that the maximum stress was 530 MPa when the thickness was 0.03 m no matter what angle the stiffening rib was. The top stress ranged from 204 MPa to 137 MPa. When the thickness was 0.01 m, the maximum stress was 1426 MPa and a 90° interval, both of which were 1329 MPa under two other kinds of conditions. Such stress far exceeds the ultimate strength of the materials. When the thickness increases from 0.01 m to 0.02 m, the stress changes significantly with a reduction amplitude of 54 %; the stress reduction amplitude is 50%~35% in the stress variation interval. When the thickness increases from 0.01 m to 0.03 m, the stress maximum reduces only 19% and the stress for two different thicknesses reduces 14%~10% within the stress variation interval. It is obvious that an increase in thickness can significantly reduce stress concentrations, but down to a certain value the reduction effect works. It should be noted that, in any arrangement, the location at the top with the maximum stress shows no obvious variations, which means it is inferred that stiffening ribs on the top with any configuration in no way reduces stress concentration values; only cost is considered to be reduced.

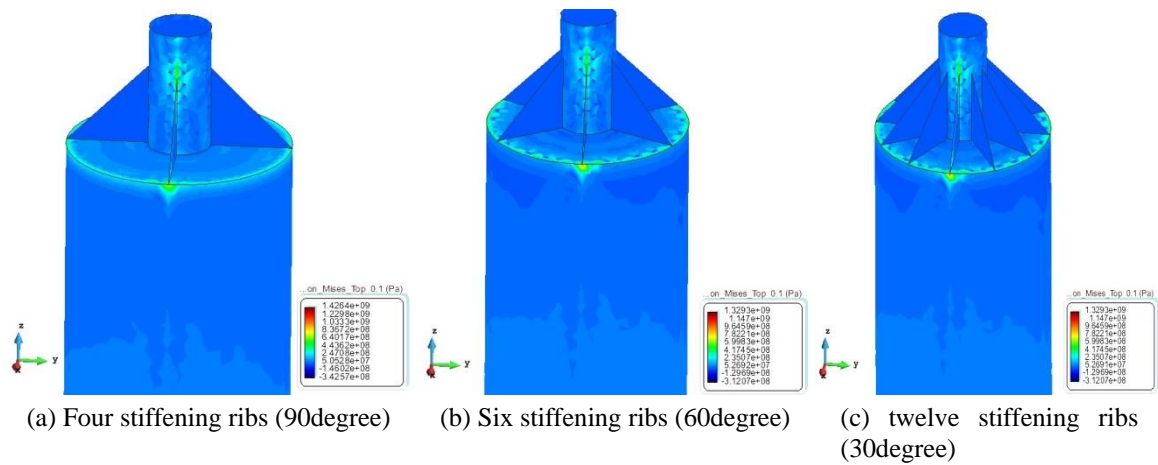


Fig. 8 The result for different ribs in load case 1 (thickness =0.01 m)

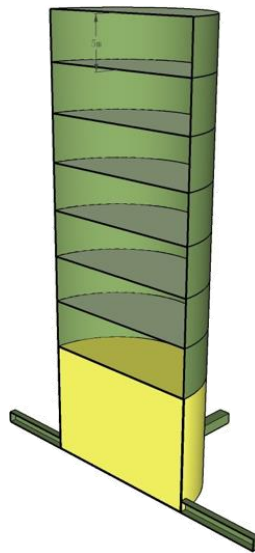


Fig. 9 Ring stiffening rib 3D

### 3.2 Internal structure arrangement of main pontoon

Pontoons are classified into the main pontoon and the spoke, this paper is primarily focused on the main pontoon. The internal structure of spoke will not be researched here. Meanwhile, it is assumed that the internal structure of the main pontoon can endure all external forces applied during the current conditions. However, the connection portion between the spoke and the main pontoon will be included within the research range.

#### 3.2.1 The ring stiffening rib

In the analysis, the thickness was set as 0.02 m, and the ring stiffening rib plane was applied in different intervals: Model 1: Applying stiffening rib plane in an interval of 5 m; Model 2: Applying

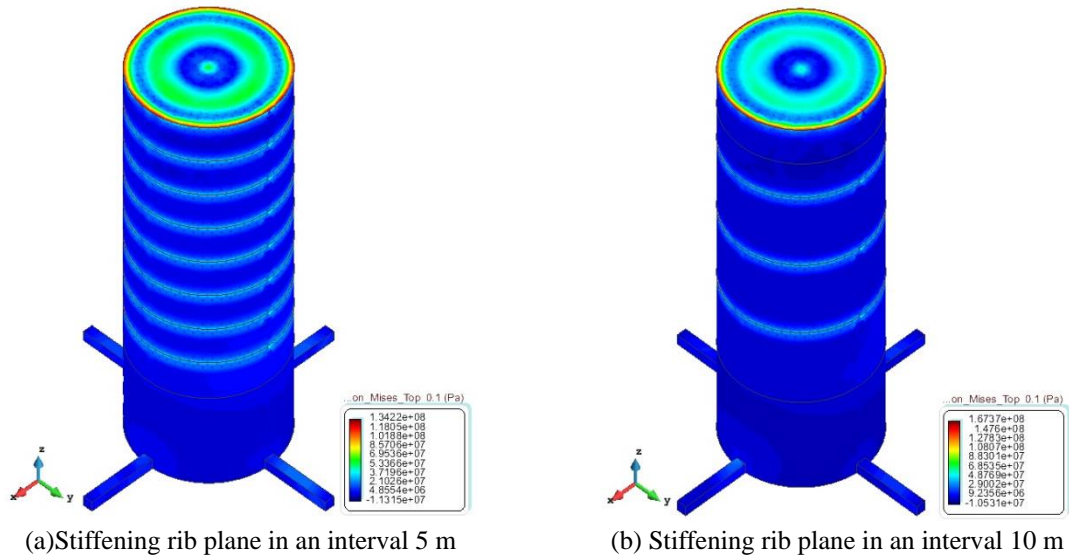


Fig. 10 Stiffening rib plane in different distance

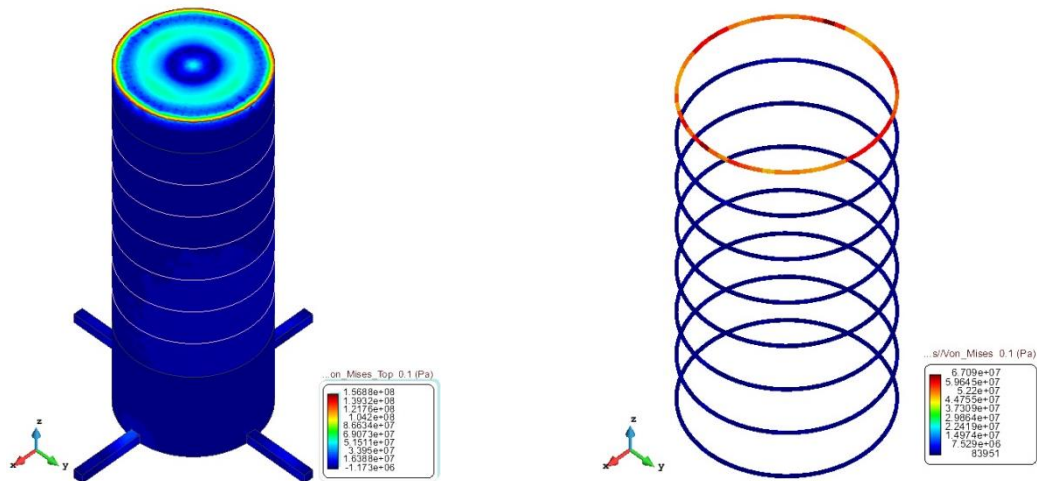


Fig. 11 Stiffening rib result in an interval 5 m and thickness of 300 mm

stiffening rib plane in an interval of 10 m; Model 3: Applying stiffening ribs in thicknesses of 300 mm or 600 mm, rather than a stiffening rib plane.

The three-dimensional graphics for them are as shown in the figure 12 below:

The result for model 1 is shown in Fig. 10, the stress result at an interval of 5 m is 134 Mpa, and the stress result at 10 m is 167 Mpa. This shows that the stress concentration reduces approximately 20% while the interval is doubled. The stress maximum occurs on the connection area between the stiffening rib plane and the pontoon. We considered using stiffening ribs to meet the proposed purpose while also reducing cost and manufacturing difficulties, because the stiffening rib plane has a high manufacturing cost. The results obtained from Model 2 are detailed in the following Fig. 11. The thickness of the stiffening rib is either 300 mm or 600 mm. In cases

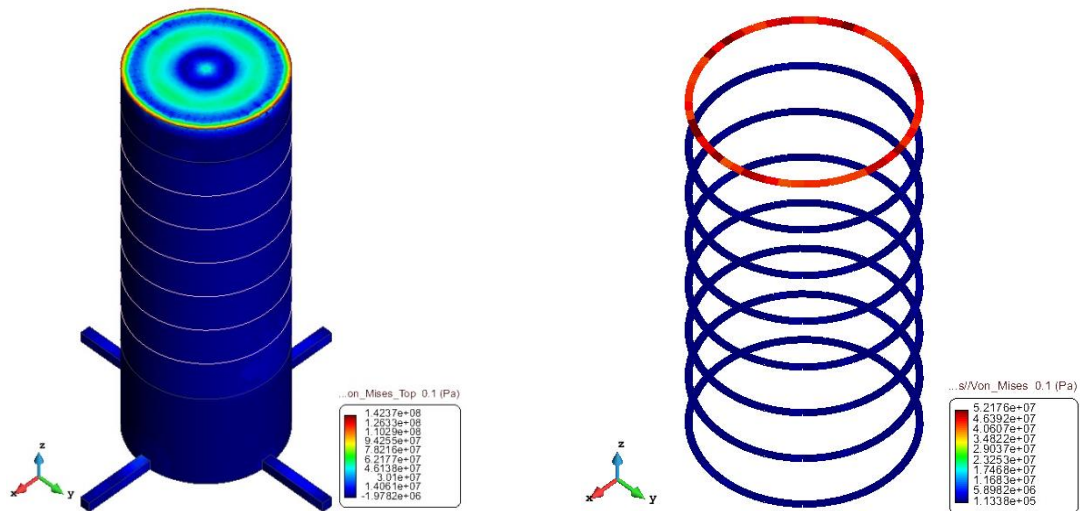


Fig. 12 Stiffening rib result in an interval 5 m and thickness of 600 mm

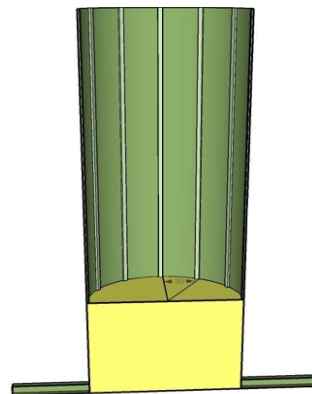


Fig. 13 Vertical stiffening rib 3D

where the application interval is 5 m, the integral stress maximum is 157 Mpa, the stress maximum shown on the stiffening rib is 67 Mpa, and the stress result of the stiffening rib, compared with the plane type stiffening, increases by 15%. Where the thickness is 600 mm, the integral stress maximum is 142 Mpa, the stress maximum shown on the stiffening rib is 52 Mpa, and the stress result of the stiffening rib, compared with the plane type stiffening, increases by 6%. Under identical interval conditions, the comparison made for stress results in the stiffening rib with thicknesses of 300 mm and 600 mm shows that the stress maximum reduces by 10% and the weight necessary for the stiffening reduces by approximately 90% while the thickness is doubled, which means the integral cost is reduced significantly.

### 3.2.2 Vertical stiffening rib

The text below reveals further research relating to the structural analysis for a vertical stiffening rib. In this case, like the above analysis, only vertical support is considered and no horizontal reinforcement support is used. The three-dimensional structure drawing is as shown in Fig. 13.

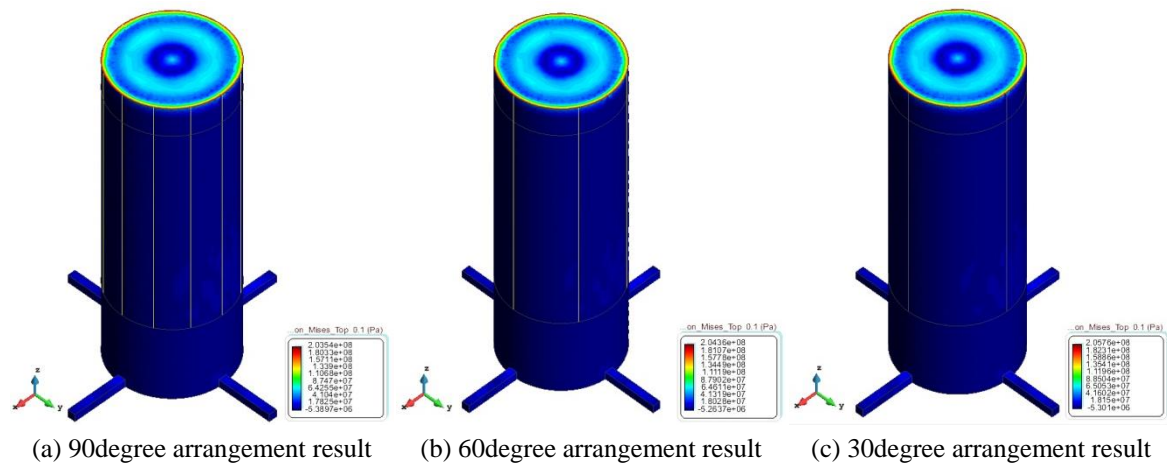


Fig. 14 The result for different vertical ribs (thickness =0.03 m)

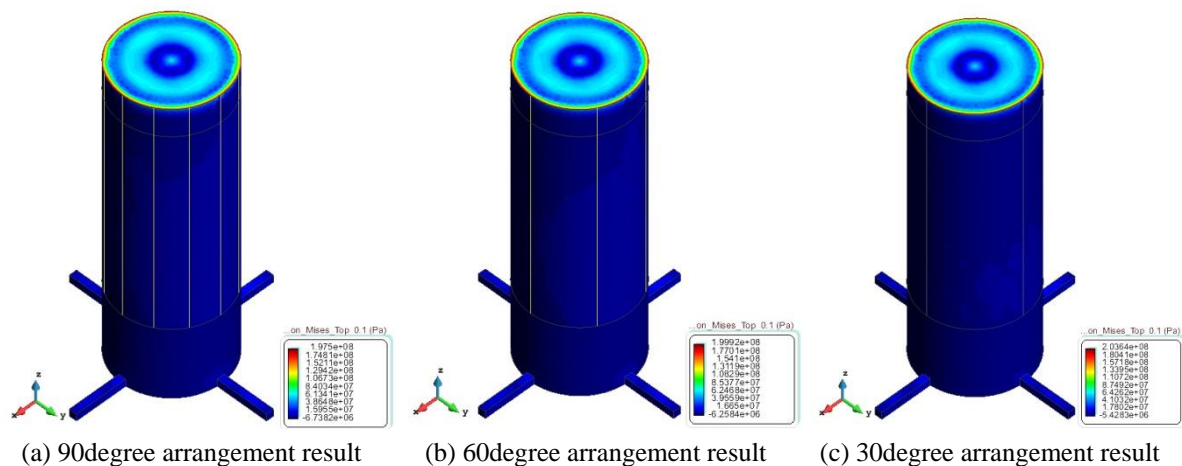


Fig. 15 The result for different vertical ribs (thickness =0.06 m)

Under the premise of applying consistent external forces, the  $H$  beam with a thickness of 300 mm and 600 mm is arranged as an integral structure by forming angles of  $30^\circ$ ,  $60^\circ$  and  $90^\circ$ . The analysis results obtained are as follows: the maximum integral stress of the structure forming the  $30^\circ$  angle is 203 MPa, the maximum integral stress of the structure forming the  $60^\circ$  angle is 204 Mpa, and the maximum integral stress of the structure forming the  $90^\circ$  angle is 206 Mpa, where the thickness maintains 300mm as shown in Fig. 17. Where the thickness is 600 mm as shown in Fig. 18, the maximum integral stress, forming  $30^\circ$ ,  $60^\circ$  and  $90^\circ$ , are 197 Mpa, 200 Mpa and 203 Mpa, respectively. The maximum stress occurs on the top, but the maximum stress varies little; the change in the angle of the vertical stiffening rib in a consistent thickness makes either little or no effect on the maximum stress.

When the stiffening rib has a thickness of 300 mm (see the nephogram below), the maximum stresses of the structure forming  $30^\circ$ ,  $60^\circ$  and  $90^\circ$  angles are 58.2 Mpa, 58.4 Mpa and 59 Mpa, respectively. There is an increasing tendency towards the maximum stress, but the increasing

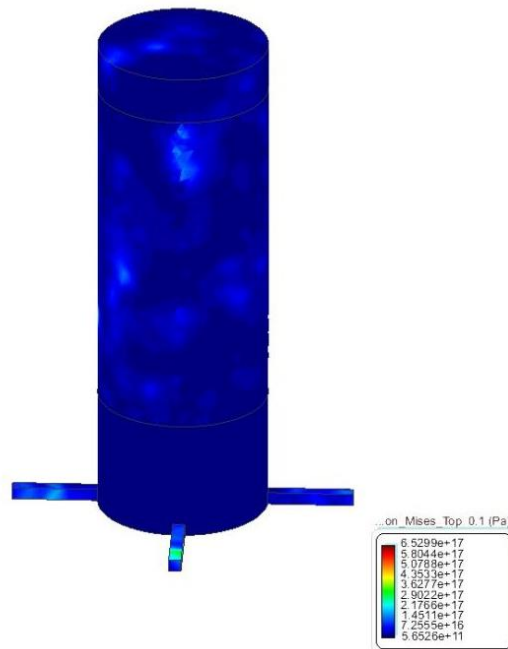


Fig. 16 Stress distribution without spoke concrete

amplitude is relatively small and may be negligible. When the stiffening rib has a thickness of 600 mm, the maximum stresses of the structure forming the 30°, 60° and 90° angles are 29.7 Mpa, 30 Mpa and 31 Mpa, respectively.

The arrangement with different angles for the vertical stiffening rib with a consistent thickness has less effect on the maximum stress. However, the maximum stress of the stiffening ribs reduces about 50% and the stresses vary more uniformly when the thickness is doubled. Compared with the *H* beam possessing a thickness of 300 mm, the *H* beam at 600 mm thick shows a uniform stress variation rather than the abrupt stress variation that occurred on the 300 mm thick *H* beam.

### 3.3 Internal structure arrangement of spoke part

A factor neglected in the analysis and calculation above is the connection portion of the main pontoon with its spoke, in which there is generally a larger stress concentration; this portion is not displayed in the photogram because the maximum stress results cover the stress values from this part. In order to better display the stress values from this section, a technical processing has been performed.

The calculated stress is far beyond the allowable stress of the material, which is liable to cause serious problems. This was never encountered in other calculations, but was attributed to the difference between the tension leg for an offshore wind turbine and for a marine structure with regard to mechanical conditions and volume. While researching the tension leg for wind power structures, further research was not conducted on the inside of spoke, since structural calculations were not involved in the study. This phenomenon will be researched further and analyzed in follow-up work. In order to mitigate the problem, we filled the spoke with concrete, and the

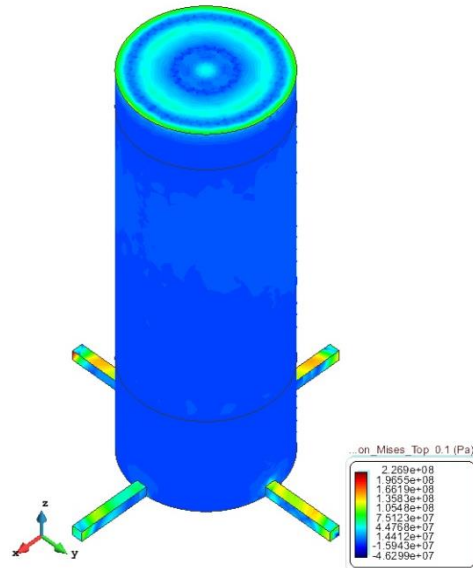


Fig. 17 Stress distribution with spoke concrete

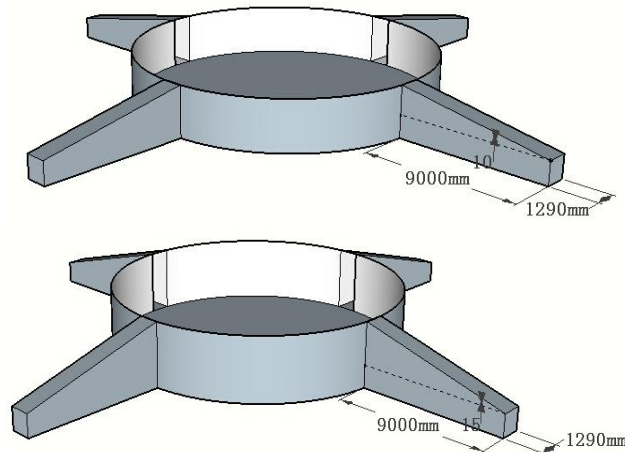


Fig. 18 Three dimension for TLP bottom in 10 degree and 15 degree

corresponding results are shown in Fig. 17 as follows:

In order to ensure the rationality of the stress results, the effects internal concrete filling had on the results will be taken into consideration in corresponding calculations while restricting it to within the material stress range, making the results analysis meaningful. A monographic study may be conducted to further probe this problem, thus it is unnecessary to further analyze it in the current study.

The above calculations show that there is a greater stress concentration on the low spoke. To deal with the possible resulting problems, the two plans below have been incorporated: (1) Under the premise of the remaining 0.02 mm thickness, we considered adapting the spoke with a variable section that was not filled with concrete. (2) The bottom original thickness dimension was

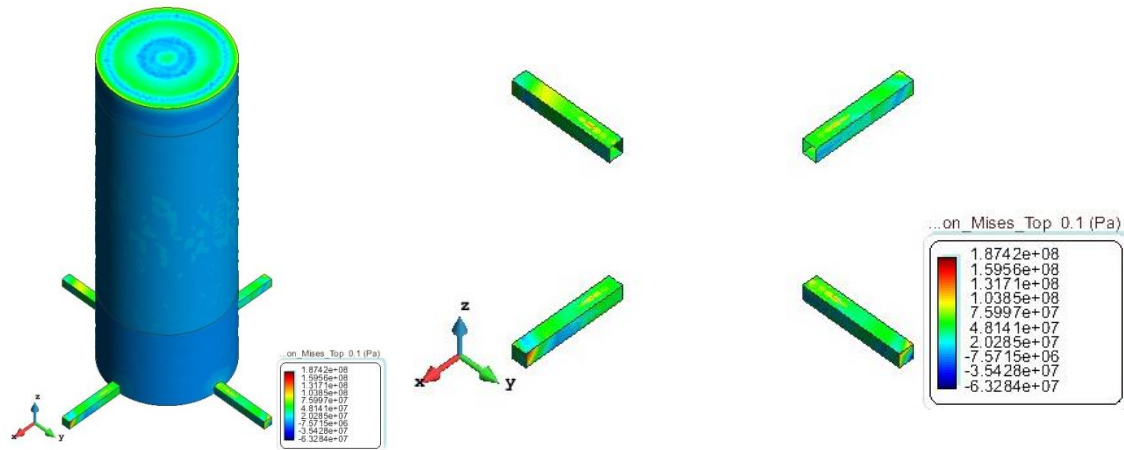


Fig. 19 Column and spoke result in zero degrees (thickness =0.03 m)

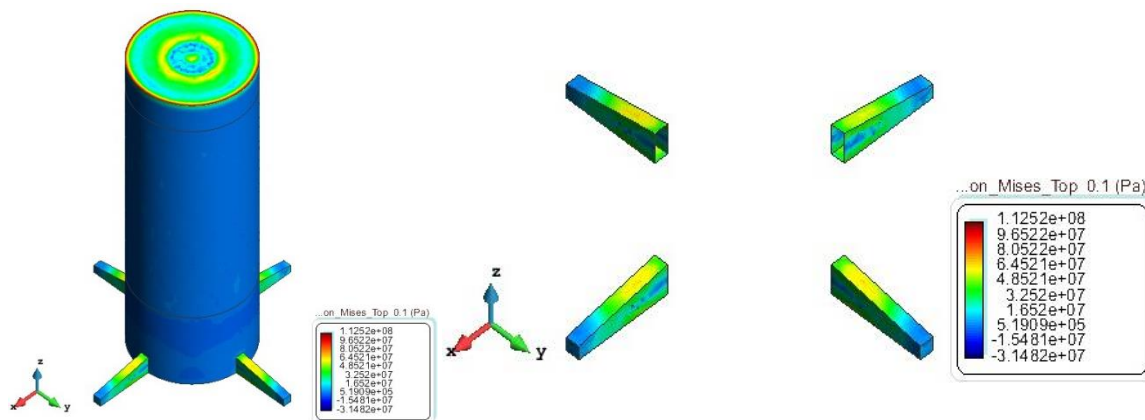


Fig. 20 Column and spoke result in 10 degrees (thickness =0.03 m)

increased from 0.02 mm to 0.03 mm, and variable section was also adapted. The dimensions of the spoke with variable sections are shown in the figures below. Given manufacturing difficulties, the bottom length was not changed, and only the oblique angle of the top was adjusted to form sections with variable sizes. The variable oblique angles used in the calculation are  $10^\circ$  and  $15^\circ$ .

After increasing the spoke's dimensions from 0.02 m to 0.03 m, the results obtained in the original dimension,  $10^\circ$  and  $15^\circ$ , are as shown in Figs. 20 and 21 below. When the spoke's thickness was increased to 0.03 m and other dimensions remained constant, the maximum stress of 187 MPa on the spoke appeared at the peripheral angle point. At the point where the spoke was increased to 0.03 m thick and arranged at  $10^\circ$  while other dimensions remained constant, the maximum stress was 112.5 MPa on the spoke. At the point where the spoke was increased to 0.03 m thick and arranged at  $15^\circ$  while the other dimensions remained constant, the maximum stress was 112.4 MPa on the spoke. In comparison, under the premise of the thickness remaining constant, the maximum stress fell by 40% where angle was increased from  $0^\circ$  to  $10^\circ$ , and stress variation was unapparent or negligible in places where the angle was increased from  $10^\circ$  to  $15^\circ$ .

The spoke's sectional dimensions were changed while keeping the thickness constant (0.02 m);

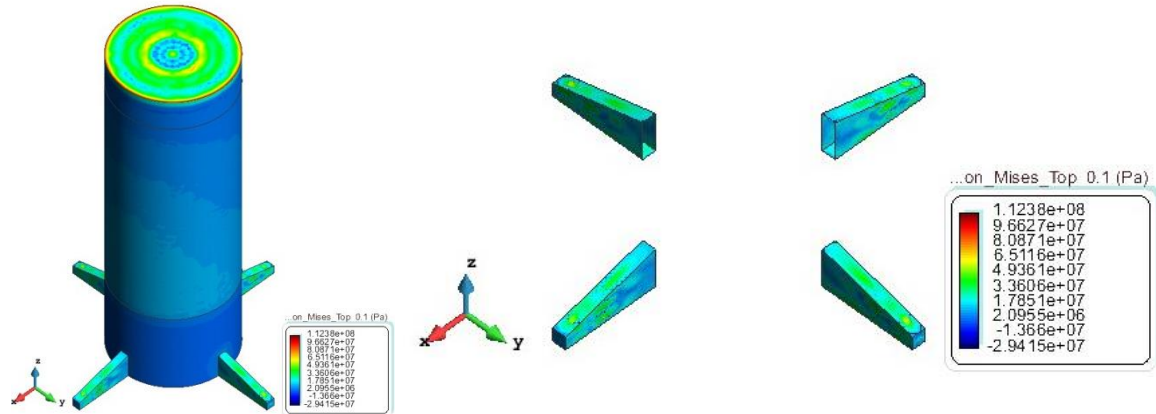


Fig. 21 Column and spoke result in 15 degrees (thickness = 0.03 m)

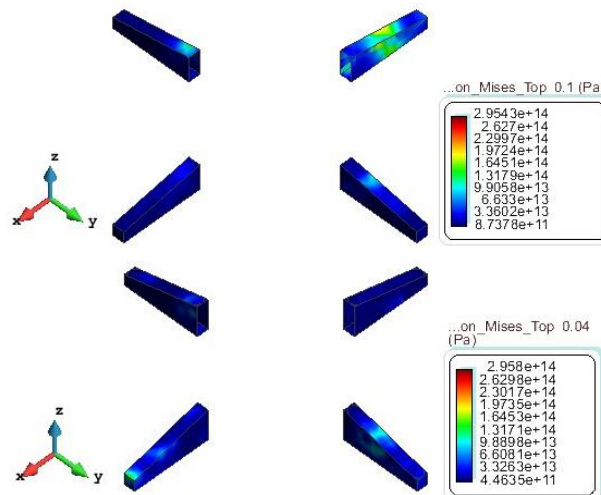


Fig. 22 Spoke result in 10&15 degrees (thickness = 0.02 m)

the stress calculation results are as shown in Fig. 22 below. The results show that the stress is far beyond the yield strength of the material, even though the order of stress magnitude was reduced where there was no concrete filled inside. Under such conditions, it is inappropriate to use a thickness of 0.02 m. A minimum thickness indicator needs to be determined.

#### 4. Conclusions

In this paper, the TLP model proposed by MIT with the 5-MW wind turbine model proposed by NREL was adopted for comprehensive consideration of wind effects, as well as wave and current combinations, in the calculation of the external additional coupling loads on a tension leg platform. The effects of these coupling loads on the variables of the tension leg internal structure were thus investigated. The following conclusions are drawn from the results of the study.

- That the maximum stress occurred at the top of the tension leg structure under the given thickness conditions is identified, and in such a case, the maximum stress has low sensitivity to the load application point. However, wall thickening will not only smoothen the maximum stress but also reduces the maximum stress, which is favorable to the utilization of materials. As a stress concentration area, the top requires subsequent local reinforcement and will not reduce or eradicate the stress concentration due to the tower rising. In order to reduce the stress on the top, when the thickness increased from 0.01 m to 0.02 m, the stress changed significantly with a reduction amplitude of 54%, and the stress reduction amplitude was 50%~35% in the stress variation intervals. When the thickness increased from 0.01 m to 0.03 m, the stress maximum reduced only 19% and the stress for the two different thicknesses reduced 14%~10% in the main stress variation intervals. It is obvious that the increase of the thickness could significantly reduce stress concentrations, but to a certain value the reduction effect works down. It should be noted that, in any arrangement, the location of the top with maximum stress shows no obvious variations, so it was inferred preliminarily that stiffening ribs on the top with any configuration in no way reduced the stress concentration value, and only cost was thought to be reduced.
- Calculation and analysis for the internal structure arrangement of the main pontoon, the stiffening rib plane at different intervals and the reinforcement at different thicknesses were analyzed. The stress concentration reduced approximately 20% when the interval was doubled. The stress maximum occurred on the connection area between the stiffening rib plane and the pontoon. In sections where the thickness was 600 mm, the maximum integral stress was 142 Mpa; the maximum stress shown on the stiffening rib was 52 Mpa, and the stress value, compared to the plane type stiffening, increased by 6%. Under identical interval conditions the comparison made for stress results of the stiffening rib at thicknesses of 300 mm and 600 mm showed that the stress maximum reduced 10% and the weight needed for the stiffening reduced approximately 90% when the thickness was doubled, significantly reducing the integral cost. When considering the vertical stiffening rib, the analysis showed that the maximum stress varied little when the thickness remained consistent; changes in the angle of the vertical stiffening rib in a consistent thickness had little or no effect on the maximum stress variation. The larger the thickness was, the lower the stress result and the higher the cost. The stress results were greater when the stiffening rib's stress results was lower and the angle was larger; however, the reduction of the maximum stress was insignificant, compared with changes to the maximum stress under conditions in which the angle was changed.
- The spoke area has been largely neglected in previous hydrodynamic studies owing to its relatively small mass and volume. The spoke for the offshore tension leg of the previous structure type did not meet the conditions for internal filling, and we therefore followed a more traditional way of thinking and considered not filling it with concrete in a preliminary study. However, the results showed that the stress was far beyond the application range of the material if the concrete has not considered. Such stress will be obviously reduced by filling the spoke with concrete. In general, the integral stiffness of the tension leg for offshore oil platforms is much greater than what is necessary for wind power structures owing to the former's larger volume, which was preliminarily inferred to be a primary cause for obvious stress variations. This phenomenon is worthy of further study and analysis in future work on the tension leg for wind power structures.

## Acknowledgments

The research described in this paper was financially supported by the Shen Zhen Strategic Development for New Industry foundation (Grant NO. JCYJ20150513151706576).

## References

- Aina, C. (2011), "Design and dynamic modeling of the support structure for a 10 MW offshore wind turbine", Master Thesis, Norwegian University of Science and Technology, Trondheim, Norway.
- Bachynski, E.E. and Torgeir, M. (2012), "Design considerations for tension leg platform wind turbines", *Marine Struct.*, **29**, 89-114
- Bae, Y.H., Kim, M.H. and Shin, Y.S. (2010), "Rotor-floater mooring coupled dynamic analysis of mini TLP-type offshore floating wind turbines", *Proceedings of the 29th International Conference on Ocean, Offshore and Arctic Engineering*, USA.
- Henderson, A.R., Argyriadis, K., Nichols, J. and Langston, D. (2010), "Offshore wind turbines on TLPs- assessment of floating support structures for offshore wind farms in German waters", *10th German Wind Energy Conference*, Bremen, Germany.
- Jonkman, J.M. (2007), *Dynamics modeling and loads analysis of an offshore floating wind turbine*, Pro Quest.
- Jonkman, J.M. (2009), "Dynamics of offshore floating wind turbines-model development and verification", *Wind Energy*, **12**, 459-492.
- Jonkman, J.M., Butterfield, S., Musial, W. and Scott, G. (2009), "Definition of a 5-MW reference wind turbine for offshore system development", *National Renewable Energy Laboratory*, Colorado, USA.
- Matha, D. (2010), "Model development and loads analysis of an offshore wind turbine on a tension leg platform with a comparison to other floating turbine concepts: April 2009", National Renewable Energy Laboratory (NREL), Golden, CO.
- Moon, W.L. and Nordstrom, C.J. (2010), "Tension leg platform turbine: a unique integration of mature technologies", *The 16th Offshore Symposium*, Texas Section of the Society of Naval Architects and Marine Engineers, Houston, Texas, February.
- Nihei, Y. and Fujioka, H. (2010), "Motion characteristics of a TLP type offshore wind turbine in waves and wind", *Proceedings of the 29th International Conference on Ocean, Offshore and Arctic Engineering*, USA.
- Pietro, J.J.M. (2009), "Structural analysis and design of floating wind turbine systems", Massachusetts Institute of Technology.
- Ren, N., Li, Y. and Ou, J. (2012a), "The effect of additional mooring chains on the motion performance of a floating wind turbine with a tension leg platform", *Energies*, **5**(4), 1135-1149.
- Ren, N., Li, Y. and Ou, J. (2012b), "The wind-wave tunnel test of a tension-leg platform type floating offshore wind turbine", *J. Renew. Sustain. Energy*, **4**(6), 063-117.
- Suzuki, K. (2009), "Development of TLP type floating structure for offshore wind farms", Technical Report, Mitsui Engineering and Shipbuilding Co., Ltd., Japan.
- Torras, S. and Diseño, J. (2011), "Cálculo y verificación de un aerogenerador marino con fondeo TLP", Master Thesis (pre-Bologna period), Universitat Politècnica de Catalunya.
- Wang, H.F. and Fan, Y.H. (2013), "Preliminary design of offshore wind turbine tension leg platform in the south china sea", *J. Eng. Sci. Tech. Rev.*, **6**, 88-92.
- Wang, H.F., Fan, Y.H. and Liu, Y. (2014), "Dynamic analysis of a tension leg platform for offshore wind turbines", *J. Power Technol.*, **94**, 42-49.
- Wayman, E. (2006), "Coupled dynamics and economic analysis of floating wind turbine systems", Master Thesis, Massachusetts Institute of Technology.
- Wayman, E.N., Sclavounos, P.D., Butterfield, S., Jonkman, J. and Musial, W. (2006), *Offshore Technology*

- Conference*, Houston, Texas, Paper No. OTC 18287.
- Withee, J.E. (2004), "Fully coupled dynamic analysis of a floating wind turbine system", Naval Postgraduate School, Monterey, California.
- Withee, J.E. (2004), "Fully coupled dynamic analysis of a floating wind turbine system", Ph.D. Thesis, MIT, Cambridge, MA, USA,
- Withee, J.E. and Sclavounos, P.D. (2004), "Fully coupled dynamic analysis of a floating wind turbine system", *Proceedings of the 8th World Renewable Energy Congress*, Denver, Colorado, USA.
- Zhao, Y.S., Jian, M.Y. and Yan, P.H. (2012), "Preliminary design of a multi-column TLP foundation for a 5-MW offshore wind turbine", *Energies*, **53**,874-3891.

CC